Chapter 2

Basic Concepts

2.1 Multidimensional Wentzel-Kramers-Brillouin (WKB) theory

Multidimensional WKB theory can be regarded as the link between quantum mechanics and classical mechanics. In particular, Chapter 3 relies on arguments of multidimensional WKB theory. Moreover, this theory facilitates the understanding of state-specific tunneling. A brief outline of multidimensional WKB theory is given in this section.

2.1.1 Invariant tori

The dynamics of a molecule of N vibrational DOF may be approximated by a system of N uncoupled harmonic oscillators for small enough total energy E. The classical Hamiltonian reads

$$H(\mathbf{p}, \mathbf{q}) = \sum_{j=1}^{N} H_j(p_j, q_j), \tag{2.1}$$

where $\mathbf{p}$ and $\mathbf{q}$ are the N-dimensional vectors of momentum and position, respectively, and $H_j(p_j, q_j)$ is the Hamiltonian of a harmonic oscillator with frequency ω_j in mass-weighted coordinates,

$$H_j(p_j, q_j) = \frac{1}{2}p_j^2 + \frac{1}{2}\omega_j^2 q_j^2. \tag{2.2}$$

The Hamiltonian H_j assumes a simple form by introducing *action-angle variables* I_j and φ_j according to

$$p_j = \sqrt{2\omega_j I_j} \cos \varphi_j, \tag{2.3}$$

$$q_j = \sqrt{\frac{2I_j}{\omega_j}} \sin \varphi_j. \tag{2.4}$$
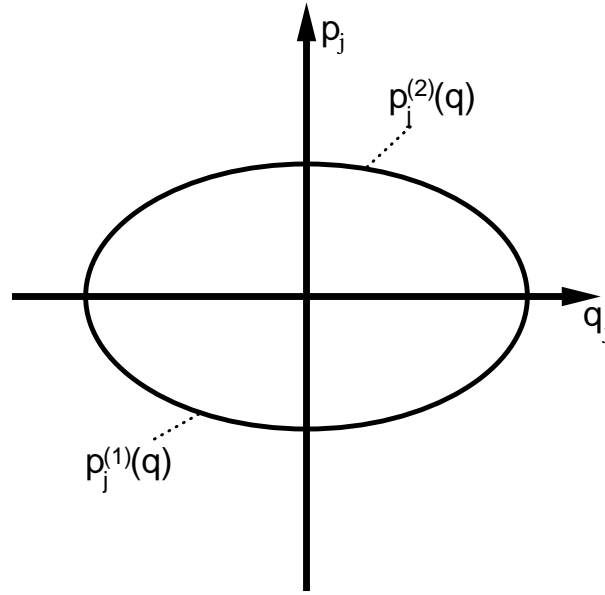
Figure 2.1: Submanifold (solid ellipse) of the phase space of the j-th harmonic oscillator for fixed action I_j. The momentum as a function of position is double-valued; the two branches $p_j^{(1)}(q_j)$ and $p_j^{(2)}(q_j)$ are marked.

The transformed Hamiltonian only depends on the actions I_j alone,

$$H_j(I_j) = \omega_j I_j. \tag{2.5}$$

Figure 2.1 depicts the phase-space (p_j, q_j) corresponding to a one-dimensional harmonic oscillator for fixed action I_j. The momentum p_j is a double-valued function of position q_j; one branch corresponds to motion with positive and negative momentum, respectively. The action I_j is given by the integral over a closed trajectory,

$$I_j = \frac{1}{2\pi} \oint p_j \, dq_j, \tag{2.6}$$

where the line integral is performed over both branches. By fixing the N actions I_j a N-dimensional submanifold Λ^N of the $2N$-dimensional phase space is selected. This submanifold is called *invariant torus* because it is invariant with respect to the dynamical transformation that generates the trajectories and it has the topology of a N-torus [49]. A N-torus is characterized by N distinct irreducible closed curves $\mathcal{C}_j$. For the two-dimensional case a 2-torus is depicted in Fig. 2.2. The closed curve $\mathcal{C}_1$ cannot be continuously deformed into $\mathcal{C}_2$ and vice-versa. Likewise, for the multidimensional case with $N > 2$.

The present system of N uncoupled harmonic oscillators is *integrable* (cf. Appendix A.1). Especially, there are N fundamental frequencies ω_j. Consider a perturbation $\tilde{H}$ added to the Hamiltonian H [Eq. (2.1)]. If the perturbation is
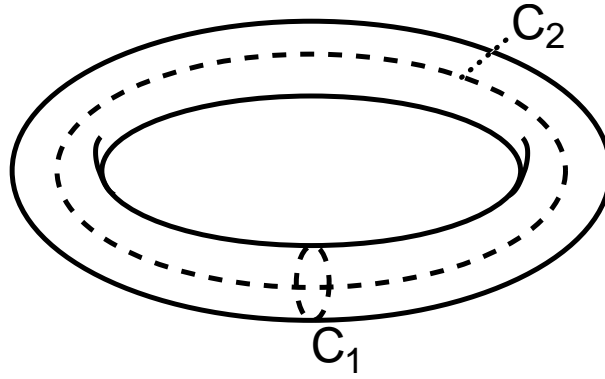
Figure 2.2: Torus of dimension 2 (schematic). Two irreducible curves, $\mathcal{C}_1$ and $\mathcal{C}_2$, are indicated by dashed lines. None of the curves can be deformed into the other without breaking. A two-dimensional invariant torus has the same topology, but it is embedded in a four-dimensional phase space.

integrable then the invariant tori are deformed without destroying their topology. If the perturbation is non-integrable (or has a non-integrable part) then the phase space of the perturbed system is still filled with invariant tori $\tilde{\Lambda}^N$. However, part of the invariant tori are destroyed and replaced by aperiodic trajectories. This was shown by numerical investigations [50].

For each position vector $\mathbf{q}$ the invariant torus $\tilde{\Lambda}^N$ associates a finite number of momentum vectors $\mathbf{p}$, i.e., there are several branches $\mathbf{p}^{(r)}(\mathbf{q})$ of the momentum vector function. For instance, in the case of N uncoupled harmonic oscillators considered above, there are 2^N branches. The line integral along any closed path $\tilde{\mathcal{C}}$ that resides solely in a single branch vanishes [49],

$$\oint_{\tilde{\mathcal{C}}} \mathbf{p}^{(r)} d\mathbf{q} = 0. \tag{2.7}$$

The path $\tilde{\mathcal{C}}$ may be a trajectory or not. Thus, the line integral along any irreducible closed curve $\mathcal{C}_k$ of $\tilde{\Lambda}^N$ is invariant with respect to any continuous deformation of that curve, i.e., there are N distinct constants of motion,

$$\tilde{I}_k = \frac{1}{2\pi} \oint_{\mathcal{C}_k} \mathbf{p} d\mathbf{q}, \tag{2.8}$$

corresponding to the irreducible closed curves. For the system of N uncoupled harmonic oscillators one has $\tilde{I}_k = I_k$ [cf. Eq. 2.6)]. For the perturbed system, the invariance guarantees that the $\tilde{I}_k$ are unique.

Equation (2.7) has another important consequence: it implies that the line integral between two points $\mathbf{q}_1$ and $\mathbf{q}_2$ is independent of the integration path, i.e., there exists a total differential on each branch,

$$dS^{(r)} = \boldsymbol{\nabla} S^{(r)}(\mathbf{q}) d\mathbf{q} = \mathbf{p}^{(r)} d\mathbf{q}, \tag{2.9}$$

where $S^{(r)}(\mathbf{q})$ is the *action function* corresponding to the r-th branch and the nabla operator is $\boldsymbol{\nabla} \equiv \partial / \partial \mathbf{q}$. The momentum of a classical trajectory,

$$\mathbf{p}^{(r)} = \boldsymbol{\nabla} S^{(r)}, \tag{2.10}$$

is always perpendicular to the surfaces of constant action. This relation is a general result of classical mechanics [51] and it applies to a larger class of submanifolds of the phase space called *Lagrange manifolds* [52, 53]. Such manifolds (including invariant tori) can be constructed by propagating a field of trajectories and collecting the values of the momenta along each trajectory given rise to a vector field $\mathbf{p}(\mathbf{q})$ of momenta, where $\mathbf{p}(\mathbf{q}) \cdot d\mathbf{q}$ is a total differential. This is called the *method of characteristics* [52, 53] (cf. Appendix A.2).

2.1.2   The Hamilton-Jacobi and transport equation

Throughout this work Hamiltonians H of the form

$$H(\mathbf{p}, \mathbf{q}) = \frac{1}{2}\mathbf{p}^2 + V(\mathbf{q}), \tag{2.11}$$

with mass-weighted Cartesian coordinates are used, where $V(\mathbf{q})$ is the PES. The corresponding time-independent Schrödinger equation with total energy E reads

$$\left[-\frac{\hbar^2}{2}\boldsymbol{\nabla}^2 + V(\mathbf{q}) \right] \Psi(\mathbf{q}) = E\,\Psi(\mathbf{q}). \tag{2.12}$$

In multidimensional WKB theory [16, 53, 30] the position representation of the wavefunction $\Psi(\mathbf{q})$ is expressed as

$$\Psi(\mathbf{q}) = \exp\{\frac{i}{\hbar}S(\mathbf{q})\}, \tag{2.13}$$

and the complex-valued function $S(\mathbf{q})$ is expanded in a power series with respect to $\hbar$,

$$S(\mathbf{q}) = S_0(\mathbf{q}) + \frac{\hbar}{i}S_1(\mathbf{q}) + \left(\frac{\hbar}{i}\right)^2 S_2(\mathbf{q}) + \ldots. \tag{2.14}$$

Inserting the *ansatz* Eq. (2.13) into the time-independent Schrödinger equation (2.12) leads together with Eq. (2.14) to an infinite set of equations for each power of $\hbar$. Only the equations corresponding to the zeroth and first order with respect to $\hbar$ are relevant for the WKB theory; the zeroth-order term S_0 determines the phase of Ψ, the corresponding zeroth-order equation reads

$$\frac{1}{2}\left(\frac{\partial S_0(\mathbf{q})}{\partial \mathbf{q}}\right)^2 + V(\mathbf{q}) = E. \tag{2.15}$$

This equation is known as the *Hamilton-Jacobi equation* (HJE) in classical mechanics [51] and S_0 is the *action* function. The first-order term S_1 determines the amplitude of Ψ, the corresponding first-order equation,

$$\sum_j \left[\left(\frac{\partial S_0}{\partial q_j} \right) \left(\frac{\partial S_1}{\partial q_j} \right) + \frac{1}{2} \frac{\partial^2 S_0}{\partial q_j^2} \right] = 0, \tag{2.16}$$

mixes zeroth-order S_0 and first-order S_1 functions. The probability amplitude $|\Psi|^2$ fulfills a continuity equation. Accordingly, Equation (2.16) is essentially a continuity equation [16, 53]. Both functions, S_0 and S_1 are in general complex-valued quantities.

Joint solutions to Eq. (2.15) and Eq. (2.16), i.e., first-order solutions, are called the WKB or semiclassical approximation to Ψ. For the one-dimensional case the derivation of such solutions is a textbook example [16]. The momentum function $p(q) = \pm \sqrt{2[E - V(q)]}$ has a positive and a negative branch. Moreover, in the classically forbidden region $V(q) > E$ the momentum is imaginary. For the connection of the wave function in the forbidden region to the wave function in the allowed region $V(q) < E$ one finds

$$\frac{C}{2\sqrt{|p|}} \exp \left\{ -\frac{1}{\hbar} \left| \int_{q_0}^{q} p \, dq \right| \right\}$$
$$\rightarrow \frac{C}{2\sqrt{|p|}} \exp \left\{ \frac{i}{\hbar} \left| \int_{q_0}^{q} p \, dq \right| - \frac{\pi}{4} \right\} + \text{c.c.}, \tag{2.17}$$

where C is a coefficient and q_0 is the classical turning point with $V(q_0) = E$. The result was derived by assuming $p(q) = \sqrt{2F_0(q - q_0)}$ near q_0, where $F_0 = -dV/dq|_{q_0}$ is the force at the turning point.

In the forbidden region (left-hand term) only the exponentially decaying term leads to a normalizable solution; in the allowed region (right-hand terms) the two branches of the momentum function $p(q)$ yield an oscillatory wave function. The prefactor $1/\sqrt{|p(q)|}$ diverges at the turning point because there one has $p(q_0) = 0$. Thus, in the vicinity of turning points the semiclassical approximation is not suitable. This is because, the de Broglie wave length h/p of a particle becomes large compared to the typical length scale of the system (for instance, the distance between two turning points of a potential well). A proper treatment of the divergence leads to an additional phase of $\pi/4$ that has to be added when connecting the wave function in the forbidden and allowed region [16].

More interesting are solution in the multidimensional case. A general theory for multidimensional semiclassical solutions was given by Maslov and Fedoriuk [52, 53] for the case of real actions. Real solutions to the HJE were discussed in Section 2.1.1: for a given invariant torus Λ^N there are branches of the action function $S^{(r)}(\mathbf{q})$. According to Eq. (2.9) these action functions are solutions to

the multidimensional HJE. Given a multidimensional solution of the HJE it is also possible to construct solutions of the transport equation Eq. (2.16) [53, 54].

A numerical implementation of the solution theory of Maslov and Fedoriuk was successfully applied to a bound state 2D system [54]. The application to multidimensional tunneling requires further approximations. This issue is addressed in Chapter 3. To this end, approximate multidimensional solutions to Eq. (2.15) in the forbidden region are required while multidimensional solutions to Eq. (2.16) are not necessary. Multidimensional and generally complex valued action functions in the forbidden region are discussed in Sections 2.1.3 and 2.1.4.

2.1.3   Complex-valued solutions of the Hamilton-Jacobi equation (HJE)

Consider an invariant torus Λ^N and a trajectory that initially moves on branch r_1 and crosses over to a neighboring branch r_2 via a particular crossing point. The projection of the relevant region of the invariant torus onto configuration space is depicted in Fig. 2.3a. There are neighboring trajectories that cross-over at different points. The collection of these points forms a surface in $\mathbf{q}$-space, the *caustic*. For convenience, the 2D case is considered, then the surface becomes a line. In 2D two caustic lines may touch at a point $\mathbf{q}_{\mathrm{hu}}$ where $V(\mathbf{q}_{\mathrm{hu}}) = E$. This situation is depicted in Fig. 2.3b. The points $\mathbf{q}_{\mathrm{hu}}$ are known as *hyperbolic umbilic points* (HU points) [30, 55]. The caustic lines touch at right angles [54] and the HU point is the origin of a local coordinate system (ξ, η), where ξ and η are directed along the two distinct caustic lines (cf. Fig. 2.3b). Near the HU point the momenta are assumed to be $p_\xi = \sqrt{2F_\xi \xi}$ and $p_\eta = \sqrt{2F_\eta \xi}$, where $F_\xi = -\partial V/\partial \xi|_{\mathrm{hu}}$ and $F_\eta = -\partial V/\partial \eta|_{\mathrm{hu}}$ are the respective forces at the HU point (local separability). Then, the semiclassical wave function near the HU point is given by a product of two one-dimensional wave functions like Eq. (2.17) [30, 55, 54],

$$\Psi(\xi, \eta) = \Psi_\xi(\xi)\, \Psi_\eta(\eta). \tag{2.18}$$

This leads to the observation that there are four quadrants around the HU point where the action $S(\xi, \eta)$ is, respectively, real-valued (R), imaginary-valued (I), and complex-valued (C_1 and C_2) [30, 55]. Likewise, there are 2^N distinct regions around a HU point of a N-dimensional system where N caustic surfaces touch.

The foregoing discussion applies to the properties of the wave function near the HU point. Thus, it is necessary to investigate the properties away from the HU points deep in the forbidden region. To this end, the complex-valued action function $S_0(\mathbf{q})$ is written as

$$S_0(\mathbf{q}) = S_R(\mathbf{q}) + i\, S_I(\mathbf{q}), \tag{2.19}$$
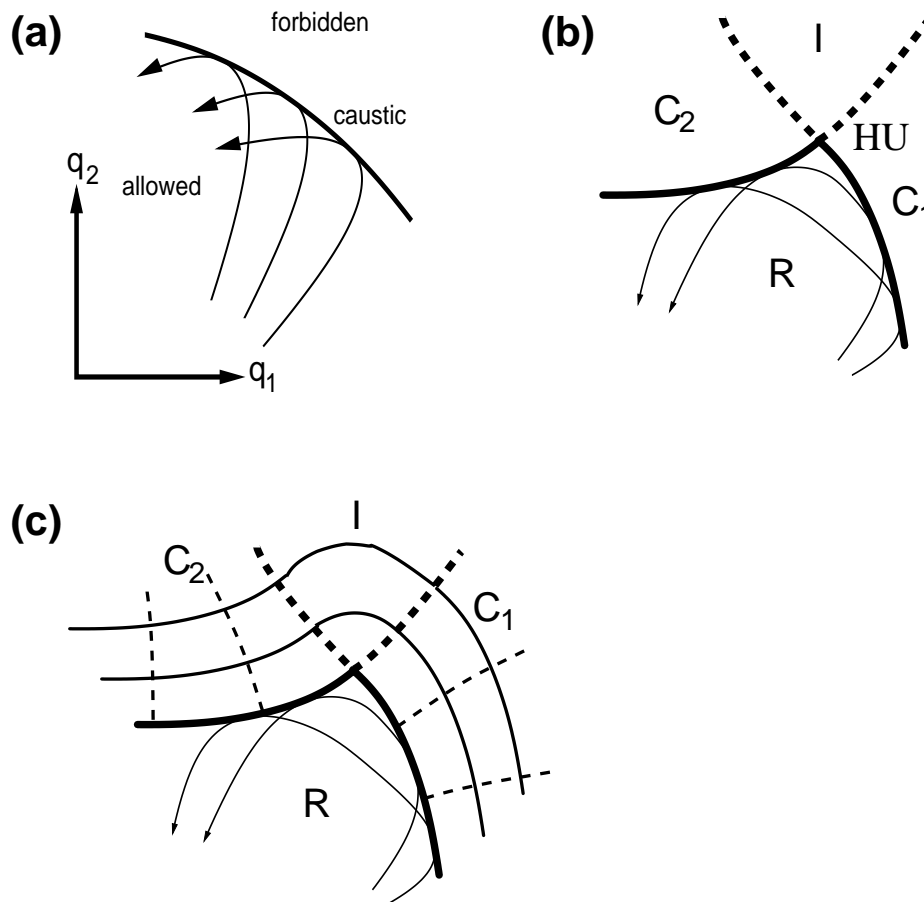
Figure 2.3: (a) Trajectories of an invariant torus Λ^2 cross from one branch to another. The projection of the crossing points onto configuration space forms a *caustic*. The caustic divides allowed and forbidden regions of configuration space. (b) Two caustics may touch in a hyperbolic umbillic (HU) point. There are four regions near the HU point. The action is real in the classically allowed (or R) region, purely imaginary in the I region, and complex in the C_1 and C_2 region. (c) Continuation of the action into the forbidden regions. Equi-amplitude (solid) and equi-phase (dashed) lines are perpendicular at any point. The amplitude and the phase is constant all-over, respectively, the R and the I region.

where S_R and S_I are the real and complex part, respectively. The HJE takes the form,

$$\frac{1}{2}\left[\left(\frac{\partial S_R(\mathbf{q})}{\partial \mathbf{q}}\right)^2 - \left(\frac{\partial S_I(\mathbf{q})}{\partial \mathbf{q}}\right)^2\right] + V(\mathbf{q}) \;\; = \;\; E, \tag{2.20}$$

$$\frac{\partial S_R(\mathbf{q})}{\partial \mathbf{q}} \cdot \frac{\partial S_I(\mathbf{q})}{\partial \mathbf{q}} = 0. \tag{2.21}$$

The second equation is required, because the PES and the energy E are real-valued quantities [56, 30]. There are surfaces of constant S_R and S_I. On the surface of constant S_R the phase of the semiclassical wave function is constant. Likewise, on the surface S_I the amplitude of the semiclassical wave function is constant (irrespective of the prefactor). Correspondingly, there are equi-phase and equi-amplitude surfaces.

The amplitude is constant all-over the allowed (or R) region since $S_I = 0$. Likewise, the phase is constant all-over the I region since $S_R = 0$. In the C regions both S_R and S_I vary. According to Eq. (2.21) the corresponding surfaces are perpendicular at any point. The expected structure of solutions of the HJE equation in all regions is depicted in Fig. 2.3c. At the boundaries of each region the corresponding surfaces smoothly join together. Especially, the caustics of the R regions join smoothly onto the equi-amplitude surfaces of the C regions. Huang *et al.* [56] gave a method to continue the equi-amplitude surface given by the R caustics into the forbidden region. Takada [57] showed that the solution of the HJE in the forbidden region indeed has the structure suggested by Fig. 2.3c (and by the method proposed by Huang *et al.*) by employing analytical continuations of the action functions $S(\mathbf{q})$ into the forbidden region.

It is possible to define classical trajectories in the I region. With $S_R = 0$, Eq. (2.20) yields after multiplication by -1 the HJE corresponding to the Hamiltonian with inverted PES at energy $-E$. The momentum $\mathbf{p} = \boldsymbol{\nabla} S_I(\mathbf{q})$ is always perpendicular to the equi-amplitude surfaces, which resembles Eq. (2.10) for the R region. Thus, the method of characteristics can be used to construct solutions S_I of the HJE in the I region by propagating classical trajectories on the inverted PES (cf. Appendix A.2).

Moreover, the I region can be extended to the minimum (the minima) of the PES. In harmonic approximation [cf. Eq. (2.1)] the total energy reads

$$E = \sum_{j=1}^{N} \hbar\omega_j(n_j + 1/2), \tag{2.22}$$

with quantum numbers n_j. One observes that the energy is proportional to $\hbar$. Thus, one can move the energy term from the HJE [Eq. (2.15)] to the transport

equation [Eq. (2.16)] and write down the new equations for the *sole I* region [58],

$$\frac{1}{2}\left(\frac{\partial S_I(\mathbf{q})}{\partial \mathbf{q}}\right)^2 = V(\mathbf{q}), \qquad (2.23)$$

$$\sum_j\left[\left(\frac{\partial S_I}{\partial q_j}\right)\left(\frac{\partial \tilde{S}}{\partial q_j}\right) - \frac{1}{2}\frac{\partial^2 S_I}{\partial q_j^2}\right] + \frac{E}{\hbar} = 0, \qquad (2.24)$$

where the amplitude function $\tilde{S}$ is introduced (sign convention according to Refs. [58, 59]). It is assumed that $\mathbf{q}$ are normal mode coordinates. In the vicinity of the minimum - where the harmonic approximation is applicable - the action is separable and given by

$$S_I(\mathbf{q}) = \sum_j \omega_j (q_j - q_j^{(0)})^2/2, \qquad (2.25)$$

where the minimum is at $\mathbf{q}^{(0)}$. For $\tilde{S}$ one finds

$$\tilde{S}(\mathbf{q}) = -\sum_j \ln|q_j - q_j^{(0)}|^{n_j} - \ln\mathcal{N}, \qquad (2.26)$$

where $\mathcal{N}$ is a normalization constant (see below). Inserting $S = iS_I - \hbar\tilde{S}/i$ into Eq. (2.13) yields for the wave function in the vicinity of the minimum,

$$\Psi(\mathbf{q}) = \mathcal{N}\prod_j (q_j - q_j^{(0)})^{n_j} e^{-\omega_j(q_j - q_j^{(0)})^2/2\hbar}. \qquad (2.27)$$

Superpositions of these wave functions are eigenstates of the harmonic oscillator (HO). Especially, for $n_j = 0$ the HO ground state is rediscovered. The harmonic approximation was already applied by using Eq. (2.22) for the total energy E. The solution Eq. (2.27) is consistent with that approximation, i.e., the wave function of the forbidden region intrinsically resembles the wave function of the allowed region in the vicinity of the minimum. To summarize: By assuming the harmonic approximation to be valid for the wave function in the allowed region [without re-distributing the energy] a global solution can be found by solving Eqs. (2.23-2.24) [with redistributing the energy]. Note, no harmonic approximation applies to the forbidden region [without redistributing the energy]. The result is contra-intuitive at first sight. However, consider the eigenfunctions of the harmonic oscillator. The shape of such a wave function is always a Hermite polynomial times a Gaussian no matter whether the classically allowed or forbidden region is studied.

2.1.4 Approximate c-valued solution of the Hamilton-Jacobi equation (HJE)

The application of results of the multidimensional WKB theory in trajectory based simulations is hampered by the fact that no trajectories can be defined in the C region [56]. Takatsuka and Ushiyama [27, 60] proposed an approximate method to

obtain *classical* trajectories in the C region. (The term classical means that these trajectories are characteristic lines corresponding to a certain HJE.) A recent review can be found in Ref. [28]. During this work the theory was reformulated [61] and it was noted that the equations of motion of the reformulated theory assume a canonical invariant form [62]. The reformulated theory is used throughout this work; it is called *TU theory*.

The one-dimensional WKB theory shows that in the classically allowed and forbidden region the momentum $p(q)$ is, respectively, real and imaginary (cf. Section 2.1.2). In the TU theory it is assumed in analogy to the 1D case that in a multidimensional system the *Cartesian* coordinates q_j are real while the conjugated momenta p_j are either real or imaginary. Real conjugated pairs $(\bar{p}_j, q_j)$ are defined by associating *parities of motion* σ_j to each DOF [27, 60],

$$p_j = \sqrt{\sigma_j}\,\bar{p}_j. \tag{2.28}$$

For $\sigma_j = +1$ and $\sigma_j = -1$ the motion is classically allowed and forbidden, respectively. Note, the transformation Eq. (2.28) is non-canonical if $\sigma = -1$. Inserting Eq. (2.28) into the Hamiltonian Eq. (2.11) yields the new Hamiltonian

$$\bar{H}(\bar{\mathbf{p}}, \mathbf{q}; \boldsymbol{\sigma}) = \sum_j \frac{\sigma_j}{2}\bar{p}_j^2 + V(\mathbf{q}), \tag{2.29}$$

where $\boldsymbol{\sigma} = (\sigma_1, \ldots, \sigma_N)$ is the vector of parities. Trajectories in the $(\bar{\mathbf{p}}, \mathbf{q})$ space can be generated by Hamilton's equation of motion,

$$\dot{\bar{p}}_j = -\frac{\partial \bar{H}}{\partial q_j} = -\frac{\partial V}{\partial q_j}, \tag{2.30}$$

$$\dot{q}_j = \frac{\partial \bar{H}}{\partial \bar{p}_j} = \sigma_j\,\bar{p}_j. \tag{2.31}$$

The first equation, Eq. (2.30), is the unchanged Newton's equation of motion. However, the second equation, Eq. (2.31), determines that for $\sigma = -1$ the velocity $\dot{q}_j$ and momentum $\bar{p}_j$ are directed in opposite directions. This formulation was shown to be equivalent to the previous formulations [61, 62], but the equations of motion Eqs. (2.30-2.31) assume a canonical invariant form. This implies that the method of characteristics (cf. Appendix A.2) can be used to construct an action function $\bar{S}(\mathbf{q}; \boldsymbol{\sigma})$ based on a fields of trajectories. However, as was noted before, the transformation Eq. (2.28) is non-canonical, i.e., trajectories generated for different sets of parities $\boldsymbol{\sigma}$ (or different *sheets* [28]) refer to different dynamical systems and it is necessary to resort to intuitive arguments in order to connect solutions belonging to different sheets.

Consider a trajectory evolving in 2D on the classical allowed sheet (all $\sigma_j = +1$) that touches a caustic line at a point $\mathbf{q}_0$ (cf. Fig. 2.4a). One may introduce a
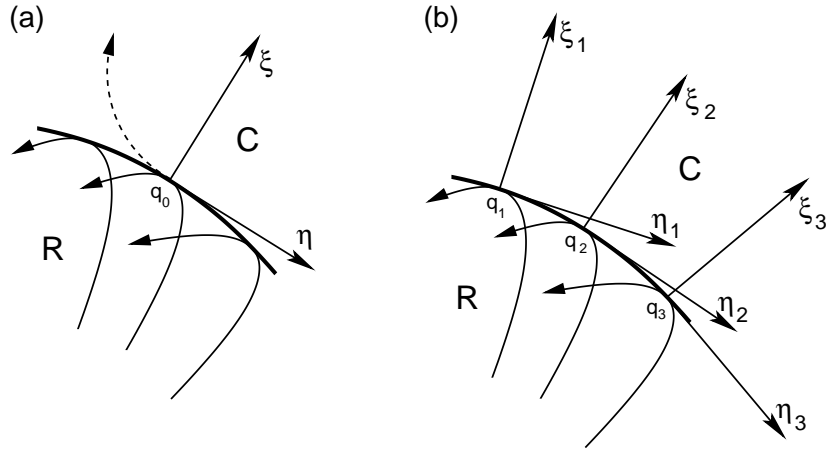
Figure 2.4: (a) Trajectories evolving on the allowed sheet $(+1, +1)$. At the crossing point $\mathbf{q}_0$ a coordinate systems (ξ, η) is introduced. The parity σ_ξ is flipped to -1 giving rise to a trajectory evolving on the sheet $(\sigma_\xi, \sigma_\eta) = (-1, +1)$ in the C region. (b) There is a coordinate system $(\xi_\lambda, \eta_\lambda)$ for each individual crossing point $\mathbf{q}_\lambda$. In general the complex vector function of collected momenta $\mathbf{p}(\mathbf{q})$ can be defined, but $\mathbf{p}(\mathbf{q})d\mathbf{q}$ is no total differential.

local coordinate system (ξ, η); ξ and η are directed perpendicular and tangent to the caustic, respectively. One observes that at $\mathbf{q}_0$ the momentum p_ξ in ξ-direction vanishes. Transformation Eq. (2.28) can be applied at this point with $\sigma_\xi = -1$ and $\sigma_\eta = +1$. This gives rise to a non-classical trajectory (dashed line) that evolves on the sheet with $(\sigma_\xi, \sigma_\eta) = (-1, +1)$ according to the Equations of Motion (2.30-2.31). Two events are possible during the course of the non-classical trajectory: The momentum of p_ξ or p_η can vanish at a certain point $\mathbf{q}'_0$ (in rare cases, the events may also occur simultaneously): (i) if $p_\xi = 0$ then transformation Eq. (2.28) can be applied again by switching σ_ξ back to $+1$ giving rise to a classical trajectory emanating from point $\mathbf{q}'_0$; (ii) if $p_\eta = 0$ then switching σ_η also to -1 yields a trajectory that evolves on the sheet with $(\sigma_\xi, \sigma_\eta) = (-1, -1)$. In this case, the Equations of motions Eq. (2.30-2.31) can be cast into

$$\ddot{\mathbf{q}} = +\frac{\partial V}{\partial \mathbf{q}}, \tag{2.32}$$

which is Newton's equation of motion for the inverted PES.

Consider the caustic of a certain invariant torus (more generally, a Lagrange manifold). A field of trajectories emanating from different points $\mathbf{q}_\lambda$ on the caustic is generated according to the present method in the C region. There is a local coordinate system $(\xi_\lambda, \eta_\lambda)$ and a distinct $(-1, +1)$ sheet associated to each point $\mathbf{q}_\lambda$. Nevertheless, it is possible to collect all values of $\mathbf{p}$ along the trajectories; this gives rise to a vector field of complex momenta $\mathbf{p}(\mathbf{q})$. In order to be a solution of

the HJE it is necessary that δS with

$$\delta S = \mathbf{p}(\mathbf{q})\, d\mathbf{q}, \tag{2.33}$$

is a total differential, i.e., any line integral over $\mathbf{p}(\mathbf{q})$ must be independent of the integration path. As a basic result of vector algebra this is the case if and only if

$$\frac{\partial p_j}{\partial q_k} = \frac{\partial p_k}{\partial q_j}. \tag{2.34}$$

This conditions cannot be fulfilled in general by the TU theory, because some momenta can be purely real while others are purely imaginary. Nevertheless, it is possible to define the action along a trajectory on a σ-sheet of the TU theory (for constant energy) by

$$S_{\mathrm{TU}}(\bar{\mathbf{p}}_0, \mathbf{q}_0, \boldsymbol{\sigma}; t) = \sum_j \int_0^t \sqrt{\sigma_j}\,\bar{p}_j(\tau)\,\dot{q}_j(\tau)\,d\tau, \tag{2.35}$$

where $(\bar{\mathbf{p}}_0, \mathbf{q}_0)$ are the initial conditions of the trajectory.

2.1.5   Semiclassical quantization

Consider an invariant torus Λ^N with N irreducible closed curves $\mathcal{C}_k$. The semi-classical quantization condition reads [49]

$$I_k = \frac{1}{2\pi} \oint_{\mathcal{C}_k} \mathbf{p}\,d\mathbf{q} = \hbar\left(n_k + \frac{\mu_k}{4}\right), \tag{2.36}$$

where μ_k are the Maslov indices [52, 49, 53]. The index counts the number of singular points (on caustics) along the irreducible closed curve $\mathcal{C}_k$. For invariant tori corresponding to deformed harmonic oscillators one has $\mu_k = 2$ in analogy to Fig. 2.1. The condition Eq. (2.36) is a generalization of the equivalent expression for the one-dimensional case and it is due to Einstein, Brillouin, and Keller (EBK) [49]. In the 1D case, it follows immediately by requiring solutions belonging to the two turning points to coincide in the allowed region [16].

The application of Eq. (2.36) assumes a quantizing invariant tori Λ^N to exist. This is in fact not guaranteed in the multidimensional case. In general the phase space of a multidimensional system can be divided into *regular* and *irregular* regions [49]. The regular regions are filled with invariant tori while the irregular regions are filled by *aperiodic* trajectories.

Consider a trajectory $(\mathbf{p}_t, \mathbf{q}_t)$ that evolves on a general invariant torus. Any observable $Z(t) \equiv Z(\mathbf{p}_t, \mathbf{q}_t)$ can be expressed as a discrete Fourier sum,

$$Z(\mathbf{p}_t, \mathbf{q}_t) = \sum_{\mathbf{m}} A_{\mathbf{n}}\,\exp\{i\Phi_{\mathbf{m}}t\}, \tag{2.37}$$

$$\Phi_{\mathbf{m}} = \sum_{j=1}^{N} m_j \omega_j, \tag{2.38}$$

where $\mathbf{m} = (m_1, \ldots, m_N)$ is a vector of N integers, $A_{\mathbf{m}}$ are the Fourier coefficients, ω_j are the N fundamental frequencies corresponding to the invariant torus, and $\Phi_{\mathbf{m}}$ are linear combinations of the frequencies. Thus, the dynamics on the torus is said to be regular. Conversely, observables corresponding to aperiodic trajectories cannot be expressed according to Eq. (2.37).

The *power spectrum* of an observable $Z(t) \equiv Z(\mathbf{p}_t, \mathbf{q}_t)$ corresponding to a trajectory $(\mathbf{p}_t, \mathbf{q}_t)$ reads [63]

$$P_{(\mathbf{p}_t, \mathbf{q}_t)}(\omega) = \frac{1}{2\pi} \lim_{T \to \infty} \frac{1}{T} \left| \int_0^T dt \, Z(t) \, \exp(-i\omega t) \right|^2. \tag{2.39}$$

If the trajectory resides in the regular region (i.e., evolves on an invariant torus), then the power spectrum is characterized by sharp peaks corresponding to the fundamental frequencies plus linear combinations thereof. If the trajectory resides in the irregular region (i.e., it is aperiodic), then the power spectrum is undefined, because the limes is non-existent. However, the finite time power spectrum exists, but depends on the propagation time. It is more convenient to average the power spectrum over a suitable ensemble of trajectories,

$$P(\omega) = \frac{1}{2\pi} \lim_{T \to \infty} \frac{1}{T} \left\langle \left| \int_0^T dt \, Z(t) \, \exp(-i\omega t) \right|^2 \right\rangle, \tag{2.40}$$

where the ensemble may be, e.g., trajectories having the same energy. Stochastic behavior of the single power spectrum corresponding to aperiodic trajectories is averaged out. Typical instants of averaged power spectra are shown in Fig. 3.10 (Chapter 3) for the 3D model of the HO_2^- anion. Power spectra similar to these are exemplary for a system with *mixed dynamics*, i.e., a system with regular and irregular regions of phase space. The prominent peaks at distinct frequencies suggest correspondence to the fundamental frequencies and the broadening is due to aperiodic motion. The existence of invariant tori was rigorously shown for small non-integrable perturbations of non-degenerate integrable systems (among further technical conditions). (An integrable system is non-degenerate if $\det \partial \omega_j / \partial I_k \neq 0$.) The theorem is named after Kolmogorov, Arnold, and Moser (KAM) [64]; sometimes invariant tori are also called *KAM tori*. Numerical investigations showed that invariant tori do exist also when the KAM theorem is not applicable [49, 50].

Adiabatic switching is a practical method to obtain a trajectory that evolves on an invariant (quantizing) torus [65]. Consider the one-dimensional Hamiltonian

$$H(p, q; \lambda) = \frac{1}{2}p^2 + \lambda \, V(q) + (1 - \lambda) \, V_0(q), \tag{2.41}$$

where $0 \leq \lambda \leq 1$ is a constant, $V(q)$ is the (anharmonic) PES, and $V_0(q)$ a PES such that the transformation from (p, q) to action-angle variables (I, φ) is *analytically* known for $H(p, q; \lambda = 0)$. Moreover, it is assumed that the canonical

transformation from (p, q) to (I, φ) exists for each λ. Thus, there is a generating function $W(q, I; \lambda)$ corresponding to the canonical transformation with (cf. Appendix A.1)

$$p = \frac{\partial W}{\partial q}, \tag{2.42}$$

$$\varphi = \frac{\partial W}{\partial I} \tag{2.43}$$

Letting $\lambda = \lambda(t)$ become a slowly varying function of t it follows that the transformed Hamiltonian reads

$$\tilde{H}(I; t) = H(I; \lambda) + \frac{\partial W}{\partial t} = H(I; \lambda) + G\dot{\lambda}, \tag{2.44}$$

where $G = \partial W/\partial \lambda$ and the dot denotes the derivative with respect to time. The function $G = G(q, I; \lambda)$ depends on q, I, λ. One can express q as a function of I and φ by inverting Eq. (2.43) with respect to q; inserting of the solution yields $G = G(\varphi, I; \lambda)$. The time evolution of I and φ are then governed by

$$\dot{I} = -\frac{\partial \tilde{H}}{\partial \varphi} = -\frac{\partial G}{\partial \varphi} \dot{\lambda}(t), \tag{2.45}$$

$$\dot{\varphi} = \frac{\partial \tilde{H}}{\partial I} = \omega(I; \lambda) + \frac{\partial G}{\partial I} \dot{\lambda}(t), , \tag{2.46}$$

where $\omega(I; \lambda)$ is the characteristic frequency of the system as a function of I and λ. The function G and its derivative - regarded as a function of t - are periodic with period $2\pi/\omega$. The integral

$$I(T) - I(0) = -\int_0^T dt \frac{\partial G}{\partial \varphi} \dot{\lambda}(t), \tag{2.47}$$

is small, if the period T is large compared to $2\pi/\omega$ and if λ is slowly varying on the time-scale given by $2\pi/\omega$. Since $\lambda(t)$ is arbitrary, this can be always fulfilled as long as $\omega \neq 0$ during the switching process.

In the multidimensional case Eq. (2.47) is replaced by

$$I_k(T) - I_k(0) = -\int_0^T dt \frac{\partial G}{\partial \varphi_k} \dot{\lambda}(t), \tag{2.48}$$

where again $G = \partial W/\partial \lambda$ and the generator function $W = W(\boldsymbol{\varphi}, \mathbf{I}; \lambda)$ depends on the vector of angles $\boldsymbol{\varphi}$ and actions $\mathbf{I}$ as well as on λ. The function G - as any observable of the system - can be expressed as a Fourier sum according to Eq. (2.37) with N fundamental frequencies ω_j [65]. That non-negligible term $A_{\mathbf{m}}$ for which the frequency $\Phi_{\mathbf{m}}$ [cf. Eq. (2.38)] is minimal determines the largest relevant period $2\pi/\Phi_{\mathbf{n}}$. The time T in Eq. (2.48) must be large compared to this period and $\lambda(t)$ must be slowly varying with respect to the time-scale defined

by this period. If there is a non-negligible term with resonant frequencies then $\Phi_n = 0$ and the adiabatic switching process fails. The numerical application of the method is hampered by very large $2\pi/\Phi_n$ corresponding to near resonant situations. Unfortunately these situations are very likely in a system with many DOF. The adiabatic switching has been successfully applied only in 1D and 2D systems.

An alternative method to obtain a trajectory that is close to an invariant torus is *normal mode sampling* [66]. It is assumed that the Hamiltonian of the system may be harmonically approximated [cf. Eq. (2.1)]. For a given set of actions $\mathbf{I}$, the momenta and positions are given by Eq. (2.3) and Eq. (2.4), respectively, where the phases φ are arbitrary. The energy of the trajectories depends on φ because the employed transformation applies exactly only to harmonic oscillators. Thus, usually the energy of a trajectory is rescaled to a desired value E simply by linear scaling of the momentum and position vector, $\mathbf{p}' = \alpha\,\mathbf{p}$ and $\mathbf{q}' = \alpha\,\mathbf{q}$, where α is the φ-dependent scaling constant. In order to verify that a certain ensemble of trajectories generated by this method is reasonable, it is necessary to investigate the corresponding ensemble averaged power spectrum.

2.2 Multidimensional tunneling

In this section general concepts of multidimensional tunneling are introduced, that are considered to be 'well-known' in the literature. These concepts are of fundamental importance for the discussion in the following Chapters.

2.2.1 Non-rigid molecules

A molecule with two symmetrically equivalent minimum geometries is considered. The molecule is non-rigid if the energy barrier $\Delta E_{\ddagger}$ between the minima and the saddle point structure is *not insuperable* [10]. Two corresponding tautomers of the molecule are interconverted by a permutation P (cf. Fig. 2.5). The saddle point geometry is invariant with respect to P. Moreover, the Hamiltonian $\hat{H}$ of the non-rigid molecule is invariant with respect P. The permutation P and the identity I form a group $\{I, P\}$ isomorphic to the point group C_s. These groups have two one dimensional representations, $+1$ and -1, respectively. Thus any eigenstate of $\hat{H}$ can be characterized to be either gerade ($+1$) or ungerade (-1) with respect to P.

Let N_{at} be the number of atoms of the molecule then the total number of DOF is $N = 3\,N_{\mathrm{at}}$. Let $\mathbf{X}$ denote a N-dimensional vector of the mass-weighted Cartesian coordinates of a certain geometry of the molecule. The center of mass
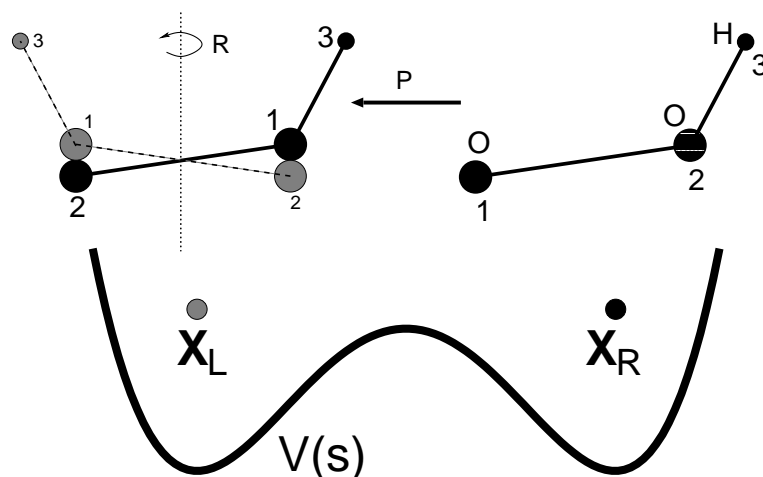
Figure 2.5: One tautomer (right-hand) is interconverted to the other tautomer (left-hand) by a permutation P. For instance, in the HO_2^- anion the two oxygen atoms are interchanged. The two structures are only unique up to an arbitrary rotation. A certain rotation R around a certain rotational axis leads to a left-hand geometry that is connected to the right-hand geometry by a rotation free path, e.g., the intrinsic reaction path (IRP) [see text for the definition]. The potential along the IRC $V(s)$ is shown, where s is the intrinsic reaction coordinate (IRC). The two unique tautomer geometries are represented by 9-dimensional vectors $\mathbf{X}_R$ and $\mathbf{X}_L$.

coincides with the origin. In the vicinity of its extrema the full-dimension *potential energy surface* (PES) $V(\mathbf{X})$ of the molecule can be harmonically approximated. For each of the three geometries among 3 infinitesimal translation and 3 infinitesimal rotation vectors (non-linear molecules) there are $N-6$ vectors $\boldsymbol{\mathcal{Y}}_j$ of dimension N corresponding to $N-6$ eigenmodes $\mathcal{Y}_j$ with eigen frequencies ω_j. The first order saddle point geometry $\mathbf{X}_{TS}$ is designated by a mode $\boldsymbol{\mathcal{Y}}_{\ddagger}^{(TS)}$ with imaginary frequency $\omega_{\ddagger}^{(TS)}$.

The PES can be characterized by the intrinsic reaction path (IRP) [67]. The IRP is the path of steepest descent starting at the saddle point geometry. The definition of the IRP reads

$$\frac{d\mathbf{X}(s)}{ds} = \frac{\boldsymbol{\nabla} V(\mathbf{X})}{|\boldsymbol{\nabla} V(\mathbf{X})|}, \qquad (2.49)$$

where s is the *intrinsic reaction coordinate* (IRC), and $\mathbf{X}(s)$ is the IRP as a function of the IRC. The integration of Eq. (2.49) starts at a geometry $\mathbf{X}_{TS} + \delta \boldsymbol{\mathcal{Y}}_{\ddagger}^{(TS)}$ infinitesimally displaced ($|\delta| \ll 1$) from the saddle point geometry in direction of the mode with imaginary frequency. The IRP ends at the minimum geometries; the minimum geometry corresponding to $\delta > 0$ and $\delta < 0$ are denoted right $\mathbf{X}_R$ geometry and left $\mathbf{X}_L$ geometry, respectively, where the terms right and left are

used for convenience. Any infinitesimal displacement along the IRP is orthogonal to any of the three infinitesimal rotations. Thus, the IRP is a rotation free path that connects the two minima via the saddle point. The two minima are related by a molecular symmetry transformation T [10],

$$\mathbf{X}_L = T\,\mathbf{X}_R, \tag{2.50}$$

where T is composed of the permutation P followed by a rotation R of the molecule, $T = R\,P$. The rotation is necessary, because $\mathbf{X}_R$ and $P\,\mathbf{X}_R$ are generally not connected by a rotation free path.

The *stable limit theorem* (*Fukui theorem*) states that the IRP reaches a minimum along the weakest mode that is symmetrically available [68]. Symmetrically available means, for instance, that for a planar molecule only in-plane modes are relevant. The energy along a typical IRP of a non-rigid molecule is depicted in Fig. 2.5 as function of the IRC. Those systems are called *double-well* systems.

In the present work, Hamiltonians of non-rigid molecules are expressed in Cartesian coordinates. The identity and the molecular symmetry transformation form a group $\{I, T\}$ isomorphic to $\{I, P\}$ (and C_s). This group is the analog for a Cartesian representation of the Hamiltonian. It is always possible to introduce Cartesian coordinates that transform according to the irreducible representations $+1$ (symmetric) and -1 (anti-symmetric). To simplify the discussion in this Section it is assumed that the reacting atom (e.g., the hydrogen of a hydrogen bond) may be described by a single large amplitude coordinate x, rotational effects are negligible, and the remaining coordinates $\mathbf{q} = (q_1, \ldots, q_{N-7})$ perform only small amplitude motions. The large amplitude coordinate must be anti-symmetric with respect to T; the other coordinates may be either symmetric or anti-symmetric.

The classical Hamiltonian in mass-weighted Cartesian coordinates reads

$$H(p_x, \mathbf{p}, x, \mathbf{q}) = \frac{1}{2}p_x^2 + \frac{1}{2}\mathbf{p}^2 + V(x, \mathbf{q}), \tag{2.51}$$

where $V(x, \mathbf{q})$ is the PES and p_x and $\mathbf{p}$ are the momenta conjugated to x and $\mathbf{q}$, respectively. The Hamiltonian - and especially the PES V - is invariant with respect to T.

2.2.2 Tunneling splittings

Consider the classical Hamiltonian H [cf. Eq. (2.1)]. A situation is assumed where there exists a quantizing invariant torus with quantum numbers $\mathbf{n}$ and energy E in the right well. The situation is depicted in Fig. 2.6 for a generic two-dimensional case. There are N constants of motion I_j. Thus, the projection of the torus onto configuration space is confined to a region inside the equi-energy
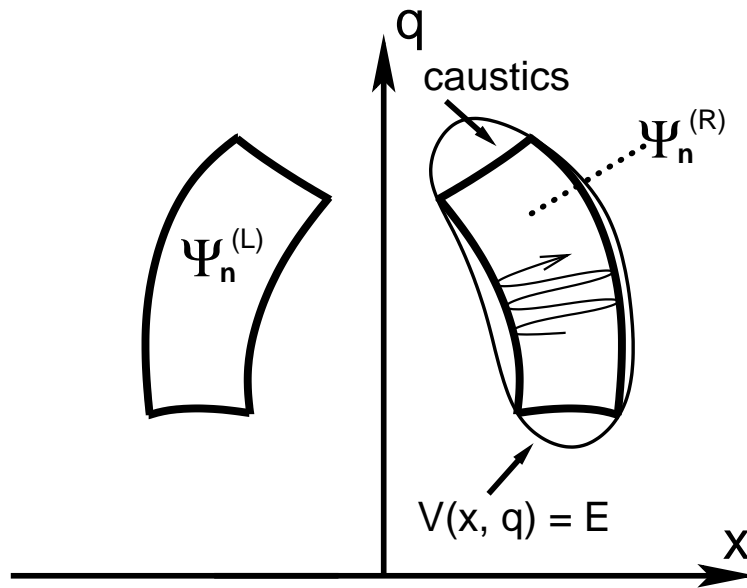
Figure 2.6: Generic double-well potential. Caustics of the right and left invariant torus are indicated by thick solid lines. The caustics tough the equi-energy line with $V(x,q) = E$ at four HU points. Semiclassical wave function $\Psi_{\mathbf{n}}^{(R)}$ and $\Psi_{\mathbf{n}}^{(L)}$ live on the right and left torus, respectively.

surface. In the two-dimensional example of Fig. 2.6 the projected torus resides inside the equi-energy line which is touched at four HU points.

The semiclassical wave function (global asymptotic approximation) corresponding to the right invariant torus is denoted as $\Psi_{\mathbf{n}}^{(R)}(x,\mathbf{q})$. Symmetry implies existence of an equivalent torus with equal energy in the left well and corresponding semiclassical wave function $\Psi_{\mathbf{n}}^{(L)}(x,\mathbf{q})$. Since the trajectories are bound to either invariant torus, a transfer from left to right and vice-versa is classically forbidden. Nevertheless, the semiclassically wave functions have exponentially decaying tails that penetrate into the respective opposite well.

The energy E of the localized invariant tori may well be above the barrier, because the existence of $N-1$ additional constants of motion confines the dynamics. This kind of barrier-less tunneling was called *dynamical tunneling* by Heller [69]. The basic properties of tunneling between tori are unaffected whether E is above or below the barrier; in principle, the invariant tori may also overlap in, e.g., configuration space [55].

Eigenstates of the corresponding quantum Hamiltonian $\hat{H}$ are either gerade or ungerade with respect to T. One can construct gerade and ungerade superpositions of the semiclassical wave functions by,

$$\Psi_{\mathbf{n}}^{+} \;=\; \frac{1}{\sqrt{2}}\left(\Psi_{\mathbf{n}}^{(R)} + \Psi_{\mathbf{n}}^{(L)}\right), \qquad\qquad (2.52)$$

$$\Psi_{\mathbf{n}}^{-} = \frac{1}{\sqrt{2}} \left(\Psi_{\mathbf{n}}^{(R)} - \Psi_{\mathbf{n}}^{(L)} \right). \tag{2.53}$$

The right-localized semiclassical wave functions is assumed to be exponentially small in the left-well and vice-versa, i.e., the semiclassical wave function are approximately orthogonal. It is expected that there are exact eigenstates $\varphi_{\mathbf{n}}^{\pm}$ that are closely resembled by the superimposed semiclassical wave functions $\Psi_{\mathbf{n}}^{\pm}$. If so, the semiclassical tunneling splitting $\Delta_{\mathbf{n}}^{(sc)}$ is given by the coupling matrix element times two, $\Delta_{\mathbf{n}}^{(sc)} = 2 \langle \Psi^{(L)} | \hat{H} | \Psi^{(R)} \rangle$.

Herring [70] showed that the semiclassical tunneling can be related to the value and gradient of the left and right wave functions along the symmetry surface Σ. In the present case a possible choice for Σ is the surface defined by $x = 0$. Consider the exact wave function $\varphi_{\mathbf{n}}^{\pm}$; they are solutions of the Schrödinger equation [Eq. (2.12)] with energies $E^{\pm}$,

$$\boldsymbol{\nabla}^2 \varphi_{\mathbf{n}}^{+} = \frac{2}{\hbar^2} \left[V - E^{+} \right] \varphi_{\mathbf{n}}^{+}, \tag{2.54}$$

$$\boldsymbol{\nabla}^2 \varphi_{\mathbf{n}}^{-} = \frac{2}{\hbar^2} \left[V - E^{-} \right] \varphi_{\mathbf{n}}^{-}. \tag{2.55}$$

Multiplication of Eq. (2.54) [Eq. (2.55)] from the left by $\varphi_{\mathbf{n}}^{-}$ [$\varphi_{\mathbf{n}}^{+}$] and integration of the difference between Eq. (2.54) and Eq. (2.55) over the half-space with $x > 0$ yields by employing Green's theorem

$$\frac{2}{\hbar^2} \left[E_{\mathbf{n}}^{-} - E_{\mathbf{n}}^{+} \right] \int_{x>0} dx \int d^{N-1} \mathbf{q} \; \varphi_{\mathbf{n}}^{+} \varphi_{\mathbf{n}}^{-}$$
$$= \int_{x=0} d^{N-1} \mathbf{q} \left[\varphi_{\mathbf{n}}^{+} \frac{\partial}{\partial x} \varphi_{\mathbf{n}}^{-} - \varphi_{\mathbf{n}}^{-} \frac{\partial}{\partial x} \varphi_{\mathbf{n}}^{+} \right], \tag{2.56}$$

where the normal vector on Σ is directed in $(-x)$-direction. Formally, this equation is exact. Inserting the superimposed semiclassical wave functions for the exact wave functions yields *Herring's formula* for the semiclassical tunneling splitting,

$$\Delta_{\mathbf{n}}^{(sc)} = \hbar^2 \int_{x=0} d^{N-1} \mathbf{q} \left\{ \Psi_{\mathbf{n}}^{(L)} \frac{\partial}{\partial x} \Psi_{\mathbf{n}}^{(R)} - \Psi_{\mathbf{n}}^{(R)} \frac{\partial}{\partial x} \Psi_{\mathbf{n}}^{(L)} \right\}, \tag{2.57}$$

where it is assumed that for $x > 0$ both products, $\Psi_{\mathbf{n}}^{(R)} \Psi_{\mathbf{n}}^{(L)}$ and $\Psi_{\mathbf{n}}^{(L)} \Psi_{\mathbf{n}}^{(L)}$, are negligible small.

Herring's formula is widely used in the literature concerning WKB theory [55, 30, 71]. It is important to note that according to Eq. (2.57) *a priori* the tunneling splitting is not related to a tunneling path, instead it is related to the properties of the wave function along a symmetry surface (or line in 2D) Σ. Moreover, as was pointed out by Benderskii *et al.* [71], if one interprets tunneling in terms of classical trajectories by means of semiclassical theory, such trajectories need to be

followed only up to Σ. Especially, these trajectories may never reach the opposite well, but, nevertheless, their contribution can be significant [72].

The interpretation of tunneling in terms of tunneling paths was, nevertheless, rather successful; for instance, generalizations of transition state theory to include tunneling paths were carried out [73]. A brief overview of related theories is given in Chapter 3.

2.2.3   Coupling types

The most simple polynomial expression of an equivalent double-well potential of a non-rigid molecule is given by the square-quartic Hamiltonian,

$$V_1(x) = -\frac{1}{2}ax^2 + \frac{1}{4}cx^4, \tag{2.58}$$

where only the large amplitude coordinate x is considered; a and c are constants that determine the two minima at $x_{\min} = \pm\sqrt{a/c}$ and the barrier height $\Delta E_{\ddagger} = a^2/4c$. The saddle point is at $x = 0$. For instance, a PES like Eq. (2.58) may serve as a simple model to describe the tunneling of a hydrogen atom in tropolone or similar molecules. A small amplitude vibration can be modeled by the harmonic oscillator PES,

$$V_2(q) = \frac{1}{2}\Omega^2 q^2, \tag{2.59}$$

where q is the corresponding small amplitude coordinate (e.g., a normal mode), and Ω is the frequency of the oscillator. If the two coordinates are coupled, the dynamics is governed by the Hamiltonian Eq. (2.1) with PES

$$V(x, q) = V_1(x) + V_2(q) + V_{12}(x, q), \tag{2.60}$$

where V_{12} is the PES coupling term. The large amplitude coordinate is anti-symmetric with respect to T while the small amplitude coordinate q can either be symmetric or anti-symmetric with respect to T. Thus, if there is a minimum at $(\bar{x}, \bar{q})$ there must be an equivalent minimum either at $(-\bar{x}, \bar{q})$ or at $(-\bar{x}, -\bar{q})$. Table 2.1 shows the three symmetrically allowed coupling terms that are at most second order in x^2 and q^2 [72]. The constant λ determines the coupling strength. The term $x\,q^2$ is not allowed by symmetry, because V_{12} must necessarily be invariant with respect to T (obviously, V_1 and V_2 are so). All three coupling types are realized in hydrogen transfer reactions of polyatomic molecules such as malonaldehyde [74] or tropolone [75, 76] (cf. Chapter 6).

The term $\lambda\,x^2\,q$ corresponds to the *symmetrical mode coupling* (SMC) case. The small amplitude coordinate (or mode) q is assumed to be symmetric with respect to the molecular symmetry transformation T. The joined potential, $V_{\text{smc}} =$
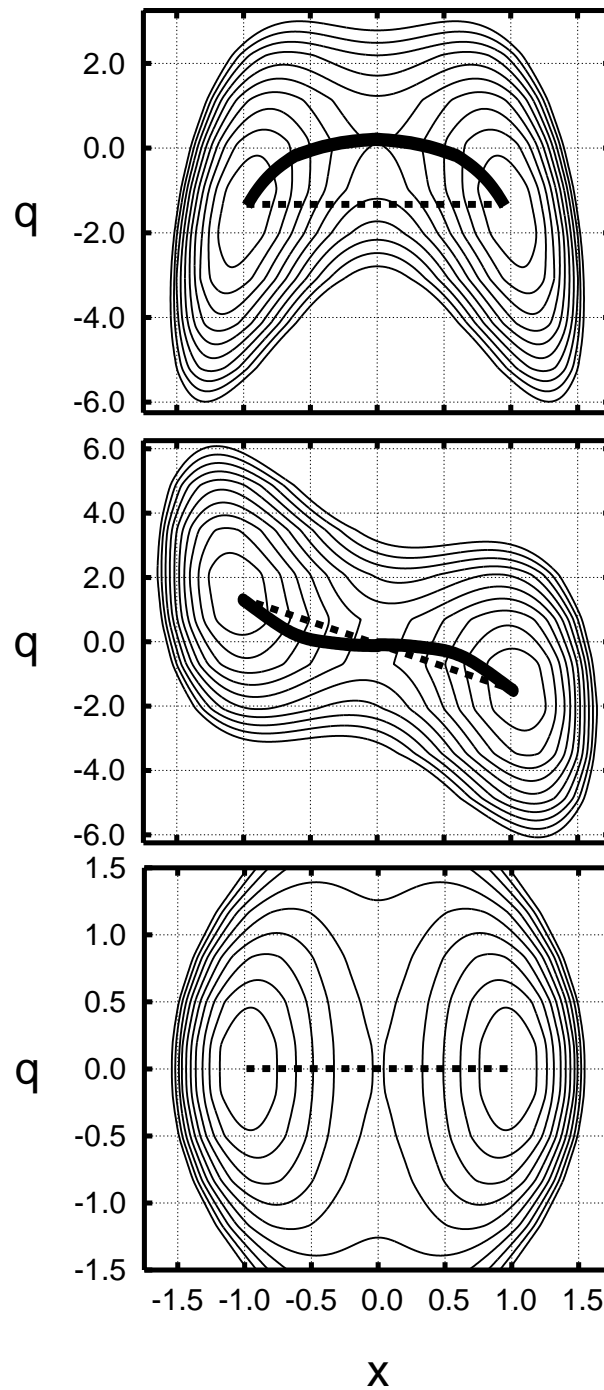
Figure 2.7: Contour plots of instances of PES showing the three coupling types (see text). The contour line spacing is 1/5 of the respective barrier height. The IRP (thick black line; schematic) and straight line paths (dashed) are indicated. *Top:* Symmetric mode coupling (SMC) [Eq. (2.61)]. The dimensionless parameters are: $a = \tilde{c} = 1$, $\Omega = 0.25$, and $\lambda = 3/32$. *Middle:* Anti-symmetric mode coupling (ASMC). The dimensionless parameters are: $a = c = 1$, $\Omega = 0.25$, and $\lambda = 0.0884$. *Bottom:* Squeezed coupling (SQZ). The dimensionless parameters are $a = c = 1$, $\Omega = 0.25$, and $\lambda = 0.2$. The straight line path coincides with the IRP.

abrev.	symmetry of q	$V_{12}(x, q)$
SMC	symmetric	$\lambda\, x^2\, q$
ASMC	anti-sym.	$\lambda\, x\, q$
SQZ	both	$\lambda\, x^2\, q^2$

Table 2.1: Symmetrically allowed coupling terms that are at most second order in x^2 and q^2. The constant λ determines the coupling strength. [(A)SMC = (anti-) symmetric mode coupling; SQZ = squeezed coupling]

$V_1 + V_2 + V_{12}$, can be written as a displaced harmonic oscillator coupled to a double-well,

$$V_{\text{smc}} = -\frac{1}{2}ax^2 + \frac{1}{4}\tilde{c}x^4 + \frac{1}{2}\Omega^2 \left(q + \frac{\lambda}{\Omega^2}\, x^2\right)^2 , \qquad (2.61)$$

with a new constant $\tilde{c} = c - 2\lambda$. The displacement of the oscillator $q^{(0)} = -\lambda x^2/\Omega^2$ is proportional to the square of x. The saddle point and minima are at $(0, 0)$ and $(\pm\sqrt{a/\tilde{c}}, -\lambda a/\tilde{c}\Omega^2)$, respectively. The barrier height is $\Delta E_{\mp} = a^2/4\tilde{c}$. Figure 2.7 (top) shows an SMC potential with typical parameters. Two characteristic paths are also given: the IRP and a straight line path connecting the minima. Trajectory (and path) based approaches for tunneling are discussed in Chapter 3. Using the symmetry relation among the left and right wave function, it is possible to rewrite Eq. (2.57) for the SMC case as

$$\Delta_{\mathbf{n}} = \hbar^2 \frac{\partial}{\partial x} \int_{x=0} d^{N-1}\mathbf{q}\, \left|\Psi_{\mathbf{n}}^{(R)}\right|^2 , \qquad (2.62)$$

where real wave functions are assumed. Positivity of the probability density implies that the integral is always positive. Moreover, reasonably a right localized wave functions must be characterized by an exponentially decaying tail in the left half of space ($x < 0$). Thus, the tunneling splitting is always positive. According to the stable limit theorem the mode with lowest frequency at the minimum is directed along the IRP. Upon excitation the tunneling splitting increases for both, the low and the high frequency mode, because the wave functions spread towards the symmetry line [cf. Figure 2.7 (top)]. However, the spreading of the low frequency mode is directed along the IRP. Therefore, the mode-selectivity of this mode is pronounced.

The term $\lambda\, x\, q$ corresponds to the *anti-symmetric mode coupling* (ASMC) case. The small amplitude coordinate q is assumed to be anti-symmetric with respect to T. The saddle point is at $(0, 0)$; the minima are at $x_{\text{min}} = \pm\sqrt{a/c + \lambda^2/c\Omega^2}$ and $q_{\text{min}} = -\lambda x_{\text{min}}/\Omega^2$. A typical PES is shown in Fig 2.7 (middle). Concerning tunneling splittings, the main properties of this coupling
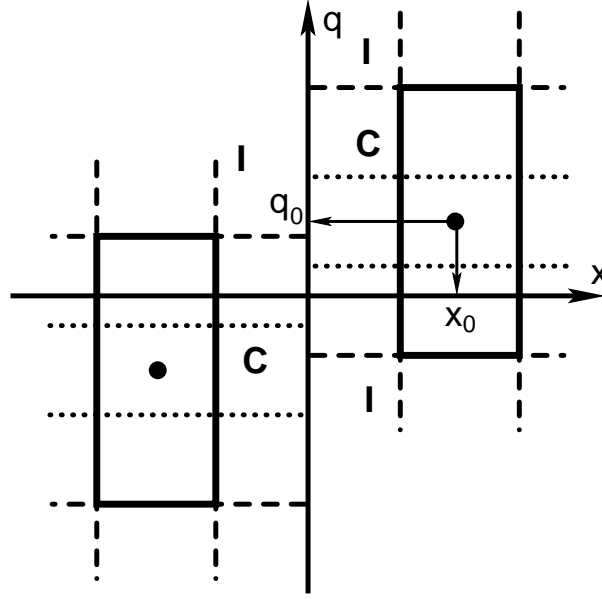
Figure 2.8: The shifted parabola model [cf. Eq. (2.63)]. Caustics of right and left invariant tori with quantum numbers $(n_x, n_q) = (0, 2)$ are indicated (solid and dashed). Dotted lines indicate nodes of the wave function. The nodes are also present in the C region. The wave function oscillates along the symmetry line Σ $(x = 0)$. The center of the two parabolas is indicated by a filled circle.

type can be most conveniently discussed by using the shifted parabola model [30]. The PES $V(x, q)$ of the shifted parabola model equals the PES of two uncoupled harmonic oscillators in the right and left well that are centered at, respectively, (x_0, q_0) and $(-x_0, -q_0)$,

$$V_{\text{spm}}(x, q) = \begin{cases} \frac{1}{2}\omega_x^2(x - x_0)^2 + \frac{1}{2}\omega_q^2(q - q_0)^2 & x > 0 \\ \frac{1}{2}\omega_x^2(x + x_0)^2 + \frac{1}{2}\omega_q^2(q + q_0)^2 & x < 0 \end{cases}, \qquad (2.63)$$

where ω_x and ω_q are frequencies corresponding to the x and q DOF, respectively. Note, in principle the discontinuity at $x = 0$ could be removed by a smooth switching function. Approximate solutions that are localized in either the right or left well are shifted harmonic oscillator eigenstates. Caustics corresponding to the invariant torus with quantum numbers $(n_x, n_q) = (0, 2)$ are depicted in Fig. 2.8. The caustics (solid and dashed) and the nodal lines (dotted) are straight lines. One observes that the wave functions oscillates along the symmetry line Σ $(x = 0)$ because the action in the C region is complex. Thus, the value of the tunneling splitting is subject to a phase cancellation phenomenon when employing Herring's formula [Eq. (2.57)]. Especially, the tunneling splitting may oscillate with respect to the quantum number n_q. This principal finding also applies to the full ASMC-PES.

The term $\lambda\,x^2\,q^2$ correspond to the squeezed coupling case. The small amplitude coordinate may either be symmetric or antisymmetric. The saddle point and minima are at $(0,0)$ and $(\pm\sqrt{a/c},0)$, respectively. A typical instance of the PES is shown in Fig. 2.7 (bottom). The joined PES can be written as an oscillator with x-dependent frequency $\omega(x)$,

$$V_{\text{sqz}} = V_1(x) + \frac{1}{2}\omega^2(x)q^2, \tag{2.64}$$

$$\omega(x) = \sqrt{\Omega^2 + 2\lambda x^2}, \tag{2.65}$$

where for $\lambda > 0$ the mode is weakened upon approaching the saddle point. The PES coupling type is typically realized for out-of-plane modes in, e.g., tropolone [76]. Upon excitation of the mode corresponding to the small amplitude coordinate (typically the weakest mode), the wave function symmetrically spreads towards the q-direction. The effective barrier for tunneling is increased and the tunneling splitting decreases. Nevertheless, Eq. (2.62) applies for the SQZ-PES, too, i.e., the tunneling splitting is always positive and the decrease is not related to a phase cancellation phenomenon.

2.3   Propagation methods

Two methods are discussed in this section, that account for the propagation of multidimensional wave packets. First, the multi-configuration time-dependent Hartree method is introduced. This method relies on a certain ansatz for the wave function and has a numerical exact limiting case. It is therefore suitable for multidimensional reference calculations. The second method is the semiclassical approximation to the quantum propagator. One may view it as the time-dependent version of the semiclassical theory (as compared to the time-independent multidimensional WKB theory discussed in Section 2.1). The *semiclassical propagator* is used in Chapter 4.

2.3.1   Multi-configuration time-dependent Hartree (MCTDH) approach

The grid-representation of a multidimensional wave function reads

$$\Psi(\mathbf{q};t) = \sum_{\nu_1=1}^{n_1} \cdots \sum_{\nu_N=1}^{n_N} C_{\nu_1,\dots,\nu_N}(t)\,\varphi_{\nu_1}^{(1)}(q_1)\cdots\varphi_{\nu_N}^{(N)}(q_N), \tag{2.66}$$

where $C_{\boldsymbol{\nu}}$ is a time-dependent coefficient matrix and $\varphi_{\nu_k}^{(k)}(q_k)$ are time-independent basis functions. The coefficient matrix scales like $\mathcal{O}(\bar{n}^N)$ with respect to the number of DOF N, where $\bar{n}$ is a typical number of basis functions for

one dimension. This exponential scaling hampers any attempt of a direct propagation of a multidimensional (say, with $N > 4$) wave function. To this end, it was proposed [77, 78, 26, 25] to resort to the multi configuration ansatz for the wave function,

$$\Psi(\mathbf{q};t) = \sum_{\nu_1=1}^{n_1} \cdots \sum_{\nu_N=1}^{n_N} A_{\nu_1,\dots,\nu_N}(t)\, \Phi_{\nu_1,\dots,\nu_N}(\mathbf{q};t), \qquad (2.67)$$

where a single configuration is given by a *Hartree product* of N time-dependent so called *single particle functions* (SPF),

$$\Phi_{\nu_1,\dots,\nu_N}(\mathbf{q};t) = \varphi_{\nu_1}^{(1)}(q_1;t) \cdots \varphi_{\nu_N}^{(N)}(q_N;t). \qquad (2.68)$$

The integers n_j refer to the number of SPF corresponding to a certain DOF q_j. Equations of motion for the coefficient matrix $A_{\nu_1,\dots,\nu_N}(t)$ and the SPF $\varphi_{\nu_j}^{(j)}(q_j;t)$ can be derived by the Dirac-Frenkel variational principle,

$$\langle \delta\Psi | \hat{H} - i\hbar\frac{\partial}{\partial t} | \Psi \rangle \overset{!}{=} 0, \qquad (2.69)$$

where the co-conditions are

$$\langle \varphi_\nu^{(j)} | \varphi_\mu^{(j)} \rangle = \delta_{\nu\mu}, \qquad (2.70)$$

$$\langle \varphi_\nu^{(j)} | \dot\varphi_\mu^{(j)} \rangle = 0. \qquad (2.71)$$

Condition (2.70) guarantees that the SPF are orthonormalized; condition (2.71) guarantees that the change of a certain SPF is orthogonal to the part of function space that is already spanned by the unchanged set of SPF. A SPF should only be changed, when the change cannot be expressed by a linear combination of the old set of SPF. The equations of motion of the *multi-configuration time-dependent Hartree* (MCDTH) method read

$$i\dot{A}_J = \sum_L \langle \Phi_J | \hat{H} | \Phi_L \rangle A_L, \qquad (2.72)$$

$$i\dot{\boldsymbol{\varphi}}^{(j)} = \left(\hat{I} - \hat{P}^{(j)} \right) \left(\boldsymbol{\rho}^{(j)} \right)^{-1} \hat{\mathbf{H}}^{(j)} \boldsymbol{\varphi}^{(j)},, \qquad (2.73)$$

where the capital letters J and L are index vectors, $\boldsymbol{\varphi}^{(j)}$ are the vectors composed of SPF of DOF j. The remaining quantities are defined by

$$\hat{P}^{(j)} = \sum_{\nu=1}^{n_j} | \varphi_\nu^{(j)} \rangle \langle \varphi_\nu^{(j)} |, \qquad (2.74)$$

$$\rho_{kl}^{(j)} = \langle \Psi | \varphi_k^{(j)} \rangle \langle \varphi_l^{(j)} | \Psi \rangle, \qquad (2.75)$$

$$\hat{H}_{kl}^{(j)} = \langle \Psi | \varphi_k^{(j)} \rangle \hat{H} \langle \varphi_l^{(j)} | \Psi \rangle, \qquad (2.76)$$

where $\hat{P}^{(j)}$ is the projector onto the space span by the SPF corresponding to DOF j, $\boldsymbol{\rho}^{(j)}$ are the single particle *density matrices*, and $\hat{\mathbf{H}}^{(j)}$ are the *mean fields*. All
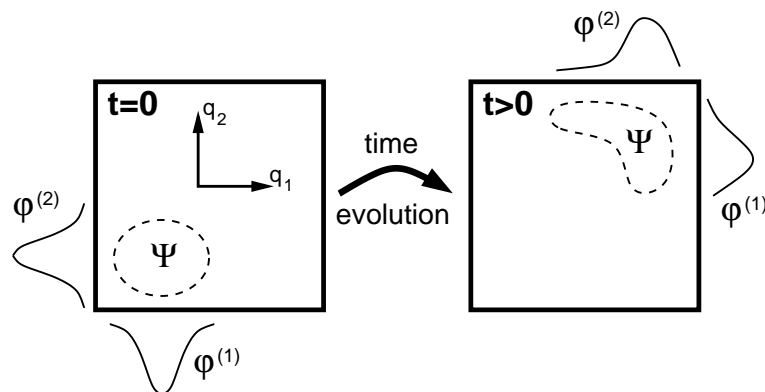
Figure 2.9: Illustration of the MCTDH method. The initial wave packet $\Psi(t = 0)$ moves and spreads during the time evolution. The time-dependent SPF $\varphi^{(k)}$ can follow the motion of Ψ (only one SPF per DOF is shown).

three quantities are related to a single DOF j only. The mean fields are operators acting on a particular DOF. The position representation of the density matrices unveils the relation to the one-particle density of a many-body system [25]. The eigenvectors and eigenvalues of $\boldsymbol{\rho}^{(j)}$ are the *natural orbitals* and *natural populations*, respectively. These quantities are unique with respect to the choice of initial SPF. The population of the highest natural orbitals provides a convergence test for the MCTDH calculation.

The time-dependent basis (i.e., a set of time-dependent SPF) can follow the wave packet during the propagation making the ansatz Eqs. (2.67-2.68) more efficient than using the same number of time-independent basis functions (cf. Fig. 2.9). The efficiency can be further increased by combining certain modes [79]. Let $\mathbf{q}^{(c_k)}$ with $1 \leq k \leq r$ denote a subset of the full coordinate vector $\mathbf{q}$. There are $r \leq N$ subsets in total and they are mutually disjoined. A modified single configuration is now given by a product of functions corresponding to the individual subsets of coordinates,

$$\tilde{\Phi}_{\nu_1,\dots,\nu_r}(\mathbf{q};t) = \varphi_{\nu_1}^{(1)}(\mathbf{q}^{(c_1)};t) \cdots \varphi_{\nu_r}^{(r)}(\mathbf{q}^{(c_r)};t). \qquad (2.77)$$

The full ansatz is obtained by replacing $\Phi \to \tilde{\Phi}$ and $N \to r$ in Eq. (2.67). For convenience the basis functions appearing in Eq. (2.77) are also denoted *single particle functions* (SPF). For a numerical integration of the equations of motion the SPF are usually expressed on a DVR grid [80, 81]. (A comprehensive review of DVR techniques is given in one of the Appendices of Ref. [25].)

The MCTDH approach is also capable of diagonalizing a multidimensional Hamiltonian [26]. First, the Hamiltonian is diagonalized within the basis of the initial SPF (providing a certain SPF guess). This yields expansion coefficients A_J

corresponding to each eigenstate. The coefficients corresponding to the desired eigenstate are used to build the quantities appearing on the r.h.s. of Eq. (2.73). Then, a small step of integration is performed for imaginary time ($t \rightarrow i\tau$) and a new optimized set of SPF is obtained. The procedure is repeated until convergence. It was shown that this method converges to the eigenstates that correspond to the variational principle applied to the MCTDH ansatz under co-condition Eq. (2.70) [26]. The method was called *improved relaxation* in order to distinguish it from a previous version, that was only able to determine the ground state.

There is a rather large number of successful applications of the MCTDH approach. For instance, a study of a 24D model of the pyranzine molecule was given [79] and recently benchmark calculations for generalized Henon-Heiles systems with up to 32 dimensions were reported [82]. However, all these systems are characterized by a single minimum. On the opposite, the present work is concerned with double minimum systems.

Extensions of the MCTDH approach were formulated [83, 84], that are heading towards the treatment of even more DOF. The multilayer formulation of Wang and Thoss [84], where each SPF is treated recursively as a MCTDH wave function, is one example.

2.3.2   The Herman-Kluk propagator

The discussion in Section 2.1 was concerned with semiclassical solutions to the time-independent Schrödinger equation. In analogy, one may ask for semiclassical solutions to the time-dependent Schrödinger equation,

$$i\hbar \frac{\partial}{\partial t} \Psi(\mathbf{q}; t) = \hat{H} \Psi(\mathbf{q}; t). \tag{2.78}$$

For time-independent Hamiltonians $\hat{H}$ the time evolution of an initial wave packet $\Psi(\mathbf{q}; t_0)$ is governed by the quantum mechanical propagator (QMP) $\hat{K}(t, t_0)$; in position representation one has

$$K(\mathbf{q}, \mathbf{q}_0; t - t_0) = \langle \mathbf{q} | \exp\{-\frac{i}{\hbar} \hat{H}(t - t_0)\} | \mathbf{q}_0 \rangle, \tag{2.79}$$

$$\Psi(\mathbf{q}; t) = \int d^N \mathbf{q}_0 \hat{K}(\mathbf{q}, \mathbf{q}_0; t - t_0) \, \Psi(\mathbf{q}_0; t_0). \tag{2.80}$$

Note, formally, the QMP is a solution of the time-dependent Schrödinger equation. Thus, it is necessary to search for the semiclassical approximation to the QMP.

Consider a canonical transformation from old variables $(\mathbf{p}, \mathbf{q})$ to new variables $(\mathbf{P}, \mathbf{Q})$ (cf. Appendix A.1). Miller [85] derived the semiclassical correspondence relation for probability amplitudes by using the *stationary phase approximation*

[31]. For the semiclassical transition probability for a system being in a state corresponding to the old canonical variable $\mathbf{q}$ (e.g., a position eigenstate) to a state corresponding to the new canonical variable $\mathbf{Q}$ (e.g., another position eigenstate) one finds

$$\langle \mathbf{q} | \mathbf{Q} \rangle = \left[-\frac{1}{(2\pi i\hbar)^N} \det \frac{\partial F_1(\mathbf{q}, \mathbf{Q})}{\partial \mathbf{q} \partial \mathbf{Q}} \right]^{1/2} \exp\left\{ \frac{i}{\hbar} F_1(\mathbf{q}, \mathbf{Q}) \right\}, \qquad (2.81)$$

where F_1 is the generator function of the canonical transformation depending on the considered variables [51].

The action along a trajectory that goes from $\mathbf{q}_0$ to $\mathbf{q}$ in time $t - t_0$ is given by the integral over the Lagrangian $\mathcal{L}$ (cf. Appendix A.1),

$$S(\mathbf{q}, \mathbf{q}_0; t - t_0) = \int_{t_0}^{t} \mathcal{L}(\mathbf{q}_\tau, \dot{\mathbf{q}}_\tau) d\tau, \qquad (2.82)$$

where the Lagrangian is the usual difference between kinetic energy T and potential energy V, $\mathcal{L} = T - V$. The action S is the F_1-type generator function of the dynamical transformation. According to its definition, it is the canonical transformation from old variables $\mathbf{q}$ at time t to new variables $\mathbf{q}_0$ at time t_0 [51], i.e., it transforms from a final point of the trajectory to its initial position. With this in mind and by using Eq. (2.81) the position representation of the semiclassical propagator reads

$$K^{(\mathrm{sc})}(\mathbf{q}, \mathbf{q}_0; t - t_0) =$$
$$\left[-\frac{1}{(2\pi i\hbar)^N} \det \frac{\partial S(\mathbf{q}, \mathbf{q}_0)}{\partial \mathbf{q} \partial \mathbf{q}_0} \right]^{1/2} \exp\left\{ \frac{i}{\hbar} S(\mathbf{q}, \mathbf{q}_0; t - t_0) \right\}. \qquad (2.83)$$

If there is more than one trajectory connecting the initial and final point in time $t - t_0$ one has to sum all the contributing trajectories in Eq. (2.83). Gutzwiller [86] derived the semiclassical propagator (also known as van Vleck-Gutzwiller propagator) as the $\hbar \to 0$ limit of the path integral [87]. Gutzwiller found [31, 86] that a phase $\phi = -in_c\pi/2$ has to be added to account for sign changes of the determinant, where n_c counts the number of points along the trajectory at which the determinant vanishes (conjugate points).

The semiclassical propagator $\hat{K}^{(\mathrm{sc})}$ is of limited use in numerical applications, because the integral involves a search for a trajectory given the two end-points and a time. This is a double-ended boundary condition. Its implementation would mean to try all possible momenta for a fixed position, which is impractical at best. The problem has been solved by resorting to initial value representations (IVR) of the propagator [88]. An IVR involves only a single integral over initial conditions of trajectories.

A numerically rather convenient IVR was derived by Herman and Kluk [34]. The method was motivated by Heller [35]. It takes advantage of the properties of generalized Gaussians (*coherent states* [32]) of the form

$$\langle \mathbf{q} | \mathbf{p}_e, \mathbf{q}_e \rangle = \left(\frac{\gamma}{\pi} \right)^{N/4} \exp\{ -\frac{\gamma}{2}(\mathbf{q} - \mathbf{q}_e)^2 + \frac{i}{\hbar}\mathbf{p}_e(\mathbf{q} - \mathbf{q}_e)\}, \qquad (2.84)$$

where N is the number of DOF, γ is an arbitrary positive parameter, $\mathbf{p}_e$ is the expectation value of the momentum operator $\hat{\mathbf{p}}$, and $\mathbf{q}_e$ is the expectation value of the position operator $\hat{\mathbf{q}}$. The properties of coherent states are summarized in Appendix B. For a fixed parameter γ they form an overcomplete set [32] and satisfy

$$\int d^N \mathbf{p}_e \int d^N \mathbf{q}_e \frac{\langle \mathbf{q}' | \mathbf{p}_e, \mathbf{q}_e \rangle \langle \mathbf{p}_e, \mathbf{q}_e | \mathbf{q} \rangle}{(2\pi\hbar)^N} = \delta(\mathbf{q}' - \mathbf{q}). \qquad (2.85)$$

By sandwiching the semiclassical propagator Eq. (2.83) using this relation twice and performing position integrals by means of stationary phase Herman and Kluk derived the equation [34]

$$\hat{K}^{\mathrm{HK}}(t - t_0) = (2\pi\hbar)^{-N} \int d^{2N}\bar{\mathbf{z}}_0 |\bar{\mathbf{z}}_t\rangle \, C_t \, e^{iS_t/\hbar} \langle \bar{\mathbf{z}}_0 |, \qquad (2.86)$$

where $\bar{\mathbf{z}} = (\bar{\mathbf{p}}, \bar{\mathbf{q}})$ has been introduced as abbreviation, $\bar{\mathbf{z}}_0$ and $\bar{\mathbf{z}}_t$ are, respectively, initial and final conditions of a classical trajectory with propagation time $t - t_0$, S_t is the action along that trajectory [cf. Eq. (2.82)], and C_t is a complex prefactor,

$$C_t = \left[\det \frac{1}{2} \left(\mathbf{M}_{pp} + \mathbf{M}_{qq} - \gamma i\hbar \mathbf{M}_{qp} + \frac{i}{\gamma\hbar}\mathbf{M}_{pq} \right) \right]^{N/2}, \qquad (2.87)$$

where the elements of the monodromy matrix were introduced,

$$\begin{pmatrix} \mathbf{M}_{pp} & \mathbf{M}_{pq} \\ \mathbf{M}_{qp} & \mathbf{M}_{qq} \end{pmatrix} \equiv \begin{pmatrix} \partial\bar{\mathbf{p}}_t/\partial\bar{\mathbf{p}}_0 & \partial\bar{\mathbf{p}}_t/\partial\bar{\mathbf{q}}_0 \\ \partial\bar{\mathbf{q}}_t/\partial\bar{\mathbf{p}}_0 & \partial\bar{\mathbf{q}}_t/\partial\bar{\mathbf{q}}_0 \end{pmatrix}. \qquad (2.88)$$

The sign of the prefactor has to be chosen in order to ensure continuity of the function C_t [89, 33]. The essence of the final result of Herman and Kluk (HK) is rather intuitive: Consider an initial wave packet $\Psi(\mathbf{q}; 0)$. The HK propagated wave packet for a later time t is obtained by propagating the center of Gaussians with a frozen width determined by γ along classical trajectories from $\bar{\mathbf{z}}_0$ to $\bar{\mathbf{z}}_t$. The contribution of each Gaussian is summed up and weighted by a factor given by the prefactor C_t, the classical phase determined by the action S_t, and the weight $\langle \bar{\mathbf{z}}_0 | \Psi(0) \rangle$. This weight can be written as $\rho \, e^{i\phi}$ with an amplitude ρ and a phase ϕ. The amplitude ρ can be conveniently used as distribution function for importance sampling (Metropolis algorithm) [90].

The HK propagator has been investigated and widely used by several authors [91, 92, 93, 94]. Moreover, it was combined with high-resolution spectral analysis

methods in order to obtain semiclassical eigenvalues [95, 39]. There are a number of different derivations known in the literature. The original derivation of Herman and Kluk is sketched here [34, 96]. More elegant treatments start from the semi-classical approximation to the representation of the propagator in coherent states $\hat{K}(\mathbf{z}, \mathbf{z}_0; t - t_0)$. Weissman [97] derived correspondence relations for so-called co-herent transformations in analogy to the results of Miller [85] for canonical trans-formations. Semiclassical approximations based on coherent states (i.e., Gaus-sians) were recently reviewed by Baranger *et al.* [33]. Especially, these authors note that the original HK formula is no strict $\hbar \to 0$ approximation. Nevertheless, the use of the original HK formula is suggested because (i) it is widely used, (ii) it essentially simple, and (iii) the error between semiclassical approximation and quantum mechanical exact solution is *analytically* known in one-dimension (see below).

Ankerhold *et al.* [98] showed that the HK propagator satisfies Schrödinger's equation up to an error operator $\hat{F}_t$,

$$i\hbar \frac{\partial}{\partial t} K^{\text{HK}} = \hat{H} \, K^{\text{HK}} + \hat{F}_t, \tag{2.89}$$

and gave an explicit expression for $\hat{F}_t$ for 1D systems. For the derivation one straightforwardly evaluates the time-derivative of the HK expression Eq. (2.86). For $t = 0$ it is possible to obtain a closed expression,

$$\hat{F}_0 = \left\langle \frac{3}{2} V(q) - \gamma V(q) \, (\hat{q} - q)^2 \right\rangle_G - V(\hat{q}), \tag{2.90}$$

where γ is corresponding HK parameter, $V(q)$ is the potential energy function, $\hat{q}$ is the position operator, and the average is defined for a function $f(q)$ as:

$$\langle f(q) \rangle_G = \sqrt{\frac{\gamma}{\pi}} \int_{-\infty}^{\infty} dq \, \exp\{-\gamma(\hat{q} - q)^2\} f(q). \tag{2.91}$$

There are two kinds of errors that make up $\hat{F}_0$: (i) the difference between semi-classical and quantum propagation and (ii) an error, that has been introduced by the approximations made in deriving the HK propagator [33]. Nevertheless, there seems to be no intuitive explanation for expression Eq. (2.90).

An analytic PES $V(q)$ can be expanded by the well-known Taylor series:

$$V(q) = V(0) + V'(0) \, q + \frac{1}{2} V''(0) \, q^2 + \frac{1}{6} V'''(0) \, q^3 + \dots, \tag{2.92}$$

where a prime means derivation with respect to q. Moreover, the average $\langle . \rangle_G$ is linear with respect to its argument. Thus, in order to determine $\hat{F}_0$ for a given PES $V(q)$ it is sufficient to determine $\hat{F}_0$ for q^n with $n = 0, 1, 2, \dots$. In Table 2.2 the corresponding error operators up to q^5 are listed. Not surprising, the $\hat{F}_0$ for at

$V(q) \rightarrow$	$q^0 \dots q^3$	q^4	q^5
$\hat{F}_0 \rightarrow$	0	$-\frac{3}{4}\gamma^{-2}$	$-\frac{15}{4}\gamma^{-2}\hat{q}$

Table 2.2: The HK error operator Eq. (2.90) at $t = 0$ for PES of the form q^n with $0 \leq n \leq 5$.

most harmonic terms ($n \leq 2$) vanish. This is because the semiclassical propagator is exact for harmonic potentials. Interestingly also $\hat{F}_0$ for the first anharmonic term q^3 vanishes [98]. The error operator for the quartic term is a constant proportional to the inverse square of the HK parameter γ. This clearly indicates, that the corresponding error is of unphysical nature, because in the derivation of the HK propagator γ was arbitrary. The same is true for the q^5 term error operator. Here, the error operator is proportional to the position operator. These observation are of particular importance in Chapter 4.

According to Eq. (2.89) the HK propagator can be separated into the exact propagator $\exp\{-\frac{i}{\hbar}\hat{H}t\}$ and an error term:

$$\hat{K}^{\text{HK}}(t) = \exp\{-\frac{i}{\hbar}\hat{H}t\} - \frac{i}{\hbar}\int_0^t \hat{F}_{t'}\,dt'. \qquad (2.93)$$

One could argue, that any non-classical effect is accounted for by the error term. However, this conclusion is incorrect. Consider the linear term in the Taylor series expansion with respect to $t = 0$,

$$\hat{K}^{\text{HK}}(t) = \hat{1} - \frac{i}{\hbar}\left(\hat{H} + \hat{F}_0\right)t + \left(\frac{i}{\hbar}\right)^2 \left(\hat{H}^2 - \frac{\hbar}{i}\frac{\partial\hat{F}_t}{\partial t}\bigg|_{t=0}\right)t^2 + \dots . \qquad (2.94)$$

It is proportional to a new operator $\hat{H}' = \hat{H} + \hat{F}_0$. Thus, for short enough time, the propagation is governed by a new time-independent Hamiltonian $\hat{H}'$. For at most quadratic terms appearing in $V(q)$ the error operator is a constant (cf. Tab. 2.2). This implies - somewhat counter-intuitive - that *all* non-classical effects are included in a 1D semiclassical HK propagation for short times with at most quadratic terms.